www.czasopisma.pan.pl PAN POLSKA AKADEMIA NAUK www.journals.pan.pl

Arch. Metall. Mater. **65** (2020), 3, 997-1000

DOI: 10.24425/amm.2020.133205

DAE-KYEOM KIM[1,2], YOUNG IL KIM[1,3], HWASEON LEE[1], YOUNG DO KIM[1,2], DONGJU LEE[3], BIN LEE[1*], TAEK-SOO KIM[1*]

GAS ATOMIZATION PARAMETRIC STUDY ON THE VIGA-CC BASED SYNTHESIS OF TITANIUM POWDER

With the recent advancement in technology for titanium metal powder injection molding and additive manufacturing, high yield and good flowability powder production is needed. In this study, titanium powder was produced through vacuum induction melting gas atomization with a cold crucible, which can yield various alloy compositions without the need for material pretreatment. The gas behavior in the injection section was simulated according to the orifice protrusion length for effective powder production, and powder was prepared based on the simulation results. The gas distribution changes with the orifice protrusion length, which changes the location of the recirculation zone and production yield of the powder. The produced powders had a spherical morphology, and the content of impurities (N, O) changed with the injected-gas purity.

Keywords: Powder production; Gas atomization; Titanium; Orifice

1. Introduction

The weight reduction of vehicles such as automobiles and aircraft has been continually studied since their development. In addition, owing to the recent paradigm shifts such as the introduction of electric cars, lightweight structural materials are attracting increasing attention. One of the most interesting lightweight structural metals is titanium (Ti), which is widely used in aerospace, defense, and medical fields because of its high strength, corrosion resistance, and biocompatibility. Furthermore, in accordance with the trend of weight reduction of automobiles, small parts such as connecting rods and bolts are actively manufactured using Ti [1-3].

Methods based on powder metallurgy are generally used to manufacture Ti parts. Among them, metal injection molding (MIM) is one of the best methods for the mass production of small precision parts through powder metallurgy. In MIM, a high-precision part is manufactured by mixing a metal powder with a binder to secure formability, forming a shape in a mold, debinding, and sintering [4]. The MIM method requires a powder consisting of spherical particles less than 100 μm in diameter. The powder should be sufficiently flowable for smooth process application, and the concentrations of impurities, such as oxygen and nitrogen, should be controlled to obtain final products with the desired physical properties. In addition to MIM, 3D printing can potentially be used to manufacture Ti parts. However, for practical applications, 3D printing requires further research to ensure flowability for easy powder use.

Ti powders for MIM and 3D printing can be prepared using various methods, such as the electrode induction melting gas atomization (EIGA), vacuum induction melting gas atomization with a cold crucible (VIGA-CC), and the plasma rotating electrode process (PREP). The EIGA, VIGA-CC, and PREP methods have advantages and disadvantages based on the characteristics of the manufacturing method. Among them, VIGA-CC has the following advantages: it does not require material pretreatment processes, such as the machining of the electrode, and it can yield various alloy compositions. Furthermore, in contrast to EIGA and PREP, this process can dissolve the scrap remaining powder production, which makes it possible to design a complementary manufacturing process [5-7].

In VIGA-CC, a spherical powder is produced by dissolving Ti in a cold crucible and spraying an inert gas. An orifice is used to control the finished Ti powder size by controlling the thickness of the molten metal. The orifices of commercial gas atomizers are made of ceramic materials, but in the case of VIGA-CC for manufacturing Ti powders, the orifice is made of tungsten, which is less reactive with molten Ti, because molten Ti reacts with

[1] KOREA INSTITUTE FOR RARE METALS, KOREA INSTITUTE OF INDUSTRIAL TECHNOLOGY, INCHEON, REPUBLIC OF KOREA
[2] HANYANG UNIVERSITY, DIVISION OF MATERIALS SCIENCE AND ENGINEERING, SEOUL, REPUBLIC OF KOREA
[3] CHUNGBUK NATIONAL UNIVERSITY, DEPARTMENT OF MATERIALS SCIENCE AND ENGINEERING, CHEONGJU, REPUBLIC OF KOREA

* Corresponding authors: lbin@kitech.re.kr, lbin@kitech.re.kr

ceramic materials. The tungsten orifice is in direct contact with the water-cooled crucible, but efficient heating of the orifice is important because molten Ti must not be cooled until it has passed through the orifice before the atomization process. Therefore, a new design is necessary for the structure of the orifice and gas-injection part. The gas behavior depends on the structure of the gas-injection part, which consists of gas-injection nozzles. For efficient powder production, it is necessary to understand the gas behavior according to the structural properties. In addition, molten Ti reacts with the atmosphere-control and injection gas, affecting the powder properties. Therefore, the characteristics of the produced powder must be analyzed with respect to changes in the injection and atmosphere-control gas.

In this study, the gas behavior at the gas-injection section was simulated according to the orifice protrusion length for effective powder production. However, because the accurate prediction of the behavior of gas-liquid metals is difficult through simulations, different powders were prepared based on gas-behavior simulations, and the efficiencies were compared. Furthermore, to achieve sufficient flowability for 3D printing, the flowability change of the powder with the change in purity of the atmosphere-control and injection gas was observed. The change in flowability was measured from the angle of repose and Hall flow rate. The microstructure of the prepared powder was observed and characterized.

2. Experimental

In this study, ANSYS Fluent 2019 R2 ACADEMIC was used to analyze the velocity distribution of gases formed according to the structure of the gas-injection nozzle. Fig. 1 schematically shows the gas-injection nozzle applied in this experiment. In order to observe the injection-gas velocity distribution according to the gas-injection nozzle structure, the simulation was performed by changing the protrusion length (h) of the molten-metal outlet orifice in the range of 2-8 mm.

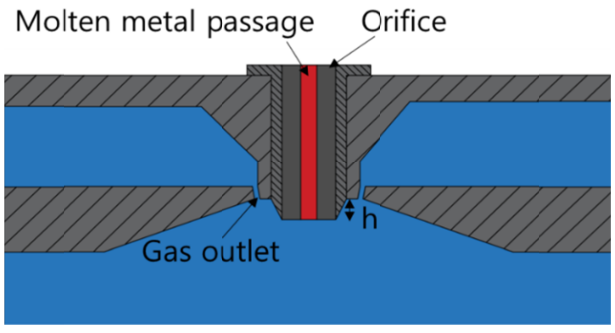

Fig. 1. Schematic of the orifice and gas-injection nozzle

VIGA-CC (Dongyang Induction Melting Furnace, Republic of Korea) was used to evaluate Ti powder production according to the gas velocity distribution. The gas-injection nozzles designed according to the orifice protrusion lengths were applied. The suction pressure for each orifice protrusion length was measured using a micro manometer (Fluker) at the top of the orifice. For powder preparation, commercially pure (CP) titanium grade 2 was used as the master alloy. The molten metal was heated to 2000°C in an Ar atmosphere, following which 2 MPa Ar gas was injected to prepare a powder. In order to evaluate powder characteristics according to the purity of the injection and atmosphere-control gas, normal-purity (99.9%) Ar and high-purity (99.999%) Ar were used to prepare different powders.

The microstructure of the powders was observed using scanning electron microscopy (SEM; JEOL Ltd., JSM-7100F) and energy-dispersive spectroscopy (EDS; JEOL). X-ray diffraction (XRD, Bruker Inc., D8 Advance) analysis was performed to confirm the crystallization of the synthesized powders. The O and N contents of the powder were evaluated using an ONH analyzer (ELTRA GmbH, ONH 2000). For the flowability characterization of the powder, the Hall flow rate (FR_H (s/50 g)) was evaluated using a Hall flow meter (HMK Test, AS-300).

3. Results and discussion

Fig. 2 shows the simulation results of gas velocity distribution with respect to the orifice protrusion length. A circulation zone is formed differently according to the orifice protrusion length at position A between the orifice and gas nozzle and at position B at the bottom of the orifice tip. Position A reduces the gas-injection efficiency by obstructing the constant gas flow from the nozzle, and position B helps form a fine powder through melt circulation.

Table 1 lists the maximum gas velocity at the orifice tip according to the orifice protrusion length. The gas velocity is 1419.73 m/s for 0 mm but decreases to 1238.85 m/s as the protrusion length increases.

TABLE 1

Orifice-tip gas velocity according to orifice protrusion length

Orifice protrusion length (mm)	Orifice Tip gas velocity (m/s)
0	1419.73
2	1389.21
4	1260.58
6	1238.85

Fig. 3 shows the results of suction pressure and powder production yield with respect to the orifice protrusion length. Powder cannot be manufactured with a protrusion length of 0 mm because of back pressure. A protrusion length of 2 mm resulted in the highest suction pressure. The simulation results show that the protrusion length of 2 mm caused back pressure owing to the large recirculation zone at position A. When the protrusion length was 4 mm, the recirculation zone at position B is large and close to the bottom of the orifice tip, creating a high suction pressure. For protrusion lengths of 6 and 8 mm, the recirculation zone is formed away from the orifice tip, resulting in a lower suction pressure [8-10].

The yield of powder production was the highest (62%) when the protrusion length was 4 mm. A high suction pressure was

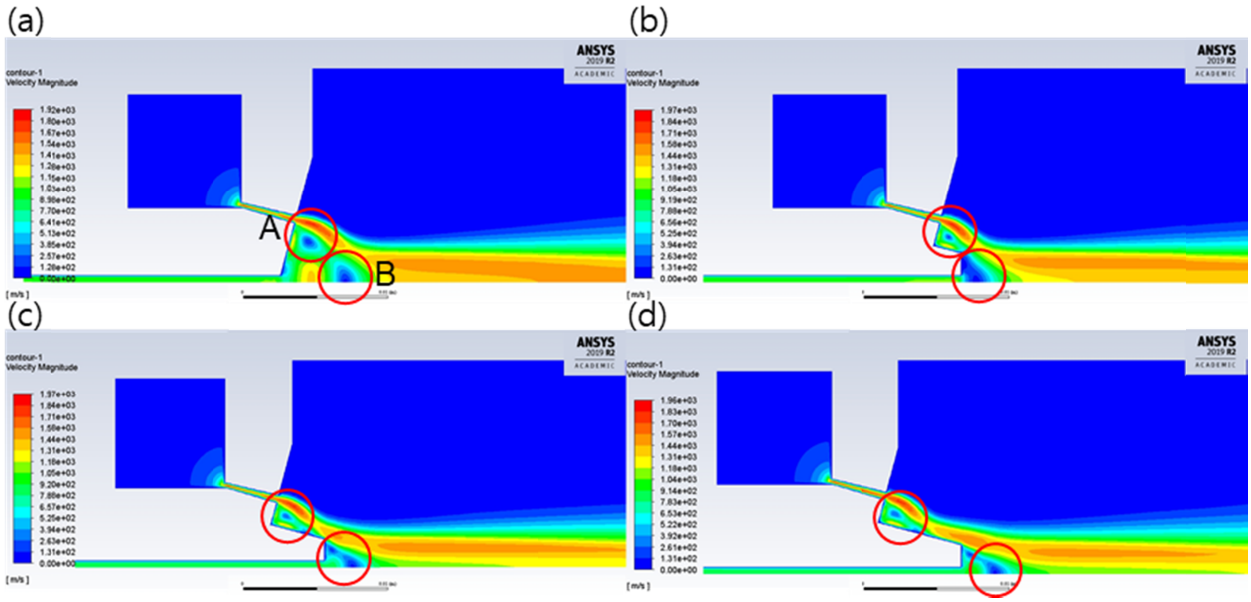

Fig. 2. Simulation results of gas-velocity distribution according to orifice protrusion length: (a) 2 mm, (b) 4 mm, (c) 6 mm, and (d) 8 mm

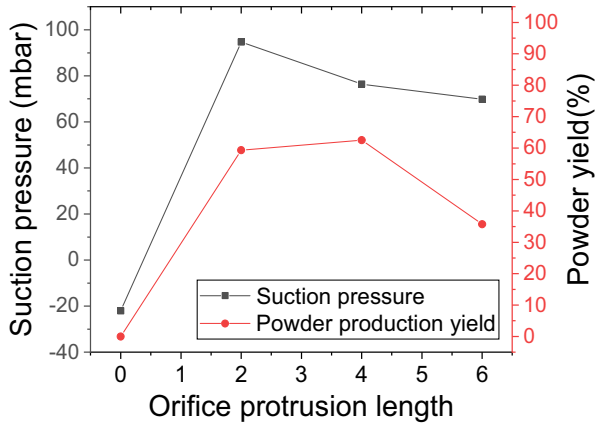

Fig. 3. Suction pressure and powder production yield according to orifice protrusion length

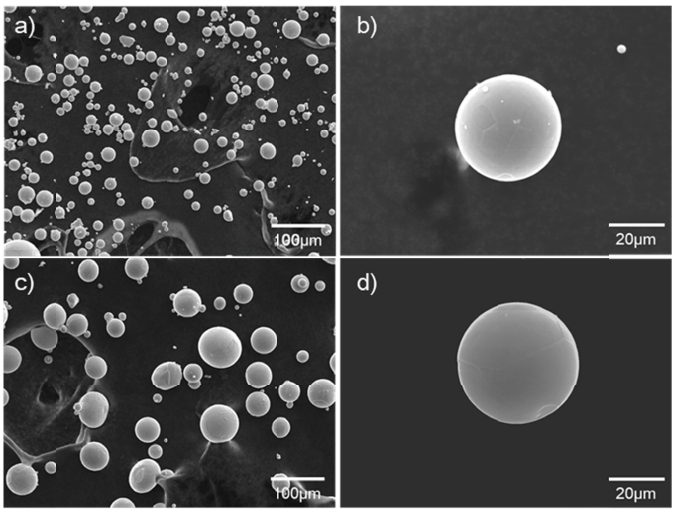

Fig. 4. SEM image of the produced powders: (a), (b) Ti powder prepared with 99.9% pure Ar gas and (c), (d) Ti powder prepared with 99.999% pure Ar gas

formed when the protrusion length was 2 mm because the ratio of gas-to-melt mass flow rate (G:M) was low and there was no recirculation zone at position B. Furthermore, the highest powder production yield was obtained when the protrusion length was 4 mm. For the case of 4 mm, recirculation occurred at position B and the suction pressure was less than that for the case of 2 mm, resulting in a high G:M. For the case of 6 mm, the powder yield was low because of the solidification of molten metal in the orifice during the atomization process [11,12].

Fig. 4 shows the morphologies of the powders prepared with different Ar gas purities in the atomization process. The powder particles are almost perfectly spherical, and the surface is smooth without any satellites or defect, irrespective of gas purity.

Table 2 lists the measurement results of nitrogen and oxygen concentrations in the prepared powders according to the Ar gas purity in the atomization process. The oxygen and nitrogen concentrations in the powder produced with normal-purity Ar gas (99.9%) are 740 ppm and 380 ppm higher than those in the powder produced with high-purity Ar gas (99.999%), respectively.

TABLE 2

Nitrogen and oxygen concentrations of powders prepared with different Ar gas purities in the atomization process

Purity of Ar gas	Prepared Ti powders	
	Oxygen	Nitrogen
	(ppm)	
99.9%	6930	1580
99.999%	6190	1200

Fig. 5 shows the XRD results of powders prepared with different Ar gas purities in the atomization process. Single-phase Ti was observed in the powder prepared with high-purity Ar, while a Ti_6O phase was observed in addition to the Ti phase with normal-purity Ar. The Ti_6O phase was generated by reaction with the oxygen contained in the injection and atmosphere-control gas [13,14].

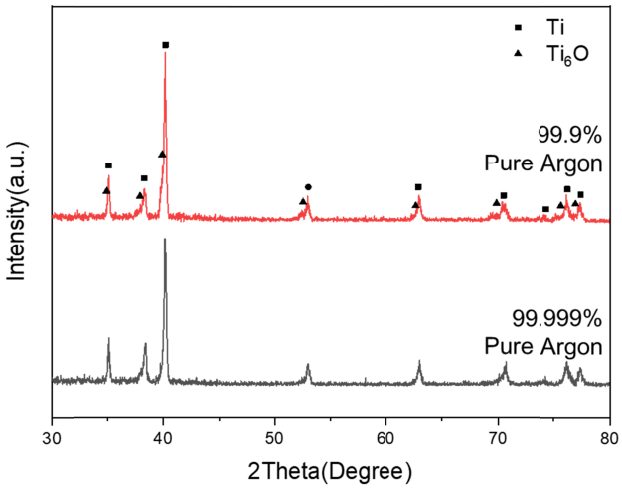

Fig. 5. XRD analysis of Ti powders prepared with different atmosphere-control and injection Ar gas purity

Table 3 lists the Hall flow rate measurement results of the powders prepared with different gas purities. The powder prepared with high-purity Ar showed a short FR_H and low angle of repose. Therefore, the powder prepared with high-purity Ar has better flowability than that prepared with low-purity Ar. The flowability decreased because hydrophilic titanium oxide, which reacts with moisture in the atmosphere, is formed on the surface of the powder prepared with low-purity Ar [15-18].

TABLE 3

Hall flow rate measurement results of powders prepared with different Ar gas purities in the atomization process

Purity of Ar gas	FR_H (s/50g)	Angle of repose (°)
99.9%	32.4	26.3
	33.4	26.6
	34.3	26.8
average	33.37	26.57
99.999%	31.9	25.5
	32.1	25.8
	32.5	25.9
average	31.17	25.73

4. Conclusions

In this study, Ti powders were prepared using VIGA-CC by optimizing the orifice protrusion length of the gas-injection part through a simulation, and the powder characteristics were measured with respect to the purity of the injection and atmosphere-control Ar gas in the atomization process. The gas distribution and recirculation-zone location change with the orifice protrusion length. The powder production yield was the highest with an orifice of 4-mm protrusion length. A recirculation zone was formed at the 4-mm orifice tip, but no solidification of the melt occurred and G:M was high. The purity of the atmosphere-control and injection gas affects the oxygen and nitrogen concentrations of the resulting Ti powder. When using normal-purity (99.9%) Ar gas, high fractions of N and O were observed in the powder, and a Ti_6O phase was formed. The shape of the powder particles was not affected by the purity of Ar gas. Higher oxygen and nitrogen concentrations in the powder reduce flowability, necessitating the use of high-purity Ar (99.999%). This result suggests that efficient powder manufacturing can be achieved by controlling the structure of gas-injection part and injection-gas purity.

Acknowledgments

This work was supported by the Industrial Strategic Technology Development Program-Development of Material Component Technology (20001221, "Development of high strength and fatigue resistance metal and manufacturing technology for root analogue dental implants") funded By the Ministry of Trade, Industry & Energy (MOTIE, Korea).

REFERENCES

[1] C. Cui, B. Hu, L. Zhao, S. Liu, Materials & Design **32**, 1684-1691 (2011).
[2] R.M. German, Materials (Basel) 6, 3641-3662 (2013).
[3] W.E. Frazier, J. of Materi. Eng. and Perform. 23, 1917-1928 (2014).
[4] G.C. Obasi, O.M. Ferri, T. Ebel, R. Bormann, Materials Science and Engineering: A 527, 3929-3935 (2010).
[5] A.J. Heidloff et al., JOM **62**, 35-41 (2010).
[6] P. Sun, Z.Z. Fang, Y. Zhang, Y. Xia, JOM **69**, 1853-1860 (2017).
[7] M. Wei, S. Chen, J. Liang, C. Liu, Vacuum **143**, 185-194 (2017).
[8] Zhao W., Cao F., Ning Z., Sun J., Transactions of Nonferrous Metals Society of China **19**, s485-s489 (2009).
[9] A.M. Mullis, A.P. Ashok Kumar, D.J. Borman, in CFD Modeling and Simulation in Materials Processing 2018 (eds. Nastac L., Pericleous K., Sabau A.S., Zhang L. & Thomas B.G.) 77-84 (Springer International Publishing, 2018).
[10] W. Strasser, F. Battaglia, in (American Society of Mechanical Engineers Digital Collection, 2016).
[11] D. Atehortua, Design, Construction and Evaluation of an Ultrasonic Gas Atomizer for Production of Aluminium Matrix Composites by Means of Osprey Process.(2008)
[12] N. Ciftci, N. Ellendt, E. Soares Barreto, L. Mädler, V. Uhlenwinkel, Advanced Powder Technology **29**, 380-385 (2018).
[13] N.M. Griesenauer, S.R Lyon, C.A. Alexander, Journal of Vacuum Science and Technology **9**, 1351-1355 (1972).
[14] K. Sakamoto, K. Yoshikawa, T. Kusamichi, T. Onoye, TISIJ International **32**, 616-624 (1992).
[15] A.B. Spierings, N. Herres, G. Levy, Rapid Prototyping Journal **17**, 195-202 (2011).
[16] A.B. Spierings, M. Voegtlin, T. Bauer, K. Wegener, Prog. Addit. Manuf. **1**, 9-20 (2016).
[17] T.-Y. Yang, S.-J. Chang, C.-C. Li, P.-H. Huang, Journal of the American Ceramic Society **100**, 56-64 (2017).
[18] B. Engel, D.L. Bourell, Rapid Prototyping Journal **6**, 97-106 (2000).